Mechanisms of heating-electrokinetic co-driven perfluorooctanoic acid (PFOA) adsorption on zeolite

Yongping Shan[1,4], Yuzhou Yin[1], Jian Wei[2], Dong Ma[1], Mingxiu Zhan[1,3], Yongguang Yin[1], Liuqing Yang[1], Wentao Jiao[1*], and Lukas Y. Wick[4]

[1] Research Center for Eco-Environmental Sciences, Chinese Academy of Sciences, 100085 Beijing, China. Email: ypshan@rcees.ac.cn

[2] State Key Laboratory of Environmental Criteria and Risk Assessment, Chinese Research Academy of Environmental Sciences, Beijing 100012, China.

[3] College of Metrology and Measurement Engineering, China Jiliang University, Hangzhou 310018, Zhejiang, China.

[4] UFZ - Helmholtz Centre for Environmental Research, Department of Environmental Microbiology, 04318 Leipzig, Germany.

[*] Corresponding author: E-mail: wtjiao@rcees.ac.cn (W. Jiao).

Abstract: Slow release of emerging contaminants limits their accessibility from soil to pore water, constraining the treatment efficiency of physio-chemical treatment sites. DC fields mobilize organic contaminants and influence their interactions with geo-matrices such as zeolites. Poor knowledge, however, exists on the joint application of heating and electrokinetic approaches on perfluorooctanoic acid (PFOA) transport in porous media. Here, we investigated electrokinetic PFOA transport in zeolite-filled percolation columns at varying temperatures. Variations of pseudo-second-order kinetic constants (k_{PSO}) were correlated to the liquid viscosity variations (η) and elctroosmotic flow velocities (v_{EOF}). Applying DC fields and elevated temperature significantly (>37%) decreased PFOA sorption to zeolite. A good correlation between η, v_{EOF}, and k_{PSO} was found and used to develop an approach interlinking the three parameters to predict the joint effects of DC fields and temperature on PFOA sorption kinetics. These findings may give rise to future applications for better tailoring PFOA transport in environmental biotechnology.

Keywords

PFOA; emerging contaminant; electrokinetic; temperature; sorption kinetics;

1. Introduction

Persistent toxic perfluorooctanoic acid (PFOA) has been detected worldwide (Flores et al., 2013; Lein et al., 2008; Lindim et al., 2015; Lorber et al., 2015), threatening the health of aquatic living, animals, and humans (Benninghoff et al., 2012; Hoffman et al., 2010; Jeon et al., 2010; Tsang et al., 2013). Although sorption and permeable reactive barrier (Qian et al., 2022) efficiently remove PFOA from the soil pore water, the slow release of PFOA from contaminated sites to pore water is prolonging and challenging risk management (Cousins et al., 2022). There is hence interest in reducing PFOA sorption from soil, to shorten the release period, especially for the high-concentration point-source soil contamination sites.

Sorption reduction in kinetics is governed by the bulk transport, film transport, and intra-particle transport steps (Tran et al., 2017), which may be regulated by electrokinetic and heating approaches. Electrokinetic phenomena are induced by external direct current (DC) electric fields allowing for the directional movement of charged particles in the electrolyte. They include the electrophoresis of charged colloidal particles (Shan et al., 2020a, 2018), the electro-migration of ions (Hunter, 2013; Sprocati and Rolle, 2022), and the electroosmotic flow of liquid (EOF). Electrokinetic technology is commonly used to clean contaminated soil sites, with the combination of surfactants, heating, etc (Ganbat et al., 2022; Niarchos et al., 2022; Wen et al., 2021). EOF, as the surface charge-driven movement of pore fluids (Elimelech et al., 1995) that can mobilize electrically neutral organic contaminants and, thereby influence their interactions with sorbents (Shan et al., 2020b). It originates from the electrical double layer in sorbent pores, and, hence, is thought to efficiently control the liquid flow in the pore networks of sorbents (Shi et al., 2008) and thereby the distribution of chemicals in the nano-size pores (Sprocati and Rolle, 2022). The electroosmotic flow velocity (v_{EOF}) is driven by the surface charge of the solid surface, the electrical double layer thickness, the width of the capillary or pore width, and the liquid viscosity (Lee et al., 2016; Probstein, 1994). And has a plug-shaped velocity profile (Grimes et al., 2000; Kar et al., 2016; Lee and Keh, 2014; Rice and Whitehead, n.d.) that allows for efficient water movement at distances as low as a few nanometers above a sorbent surface. It has been found to reduce the sorption of electrically neutral oil

contaminant phenanthrene (PHE) in geo-sorbents (silica, zeolite, and Al_2O_3) (Shan et al., 2020b) or to increase dissolution and release of alginate-embedded solid PHE by 120-times as compared to stagnant water conditions (Shi et al., 2008).

Temperature is another driver of the chemical sorption capacity of sorbents and the kinetics of chemical sorption to sorbents, respectively (Do, 1998). The sorption capacity describes the temperature-dependent equilibrium loading of adsorbate to sorbents and is often approximated by Langmuir and Freundlich sorption models (Do, 1998). The sorption kinetics reflects the sorption rate over time and is commonly described by kinetic sorption models, including the intra-particle model, the pseudo-first-order (PFO), and the pseudo-second-order (PSO) model (Kopinke et al., 2018; Tran et al., 2017). Finally, temperature also influences the viscosity (η) as a further driver of chemical diffusion and electroosmotic flow velocity (Ghosal, 2004).

Poor knowledge however exists on the joint application of heating and electrokinetic approaches on PFOA transport and sorption in porous media. With a pKa of 0-1 (Goss, 2008), PFOA will be predominantly deprotonated at neutral pH. Electrokinetic PFOA transport and sorption thus will be driven by EOF, sorption strength, and environmental conditions such as temperature. Here, we investigated electrokinetic PFOA transport in zeolite-filled percolation columns at pH = 7, yet varying temperatures, calculated PFOA pseudo-second-order (PSO) kinetic constants (k_{PSO}) of PFOA sorption to zeolite and correlated them to viscosity changes (η) and calculated EOF velocities (v_{EOF}). We also addressed the following questions: i) what are the effects of DC electric fields and temperature on the transport and sorption of PFOA to zeolites? (ii) what are the driving factors of possible synergetic effects? and (iii) can the effects be predicted?

2. Material and Methods

2.1 Reagents and sorbents

Perfluorooctanoic acid (PFOA, Sigma-Aldrich, USA) was diluted with DI water to prepare the storage solution for sorption experiments. PFOA standard (100 µg/mL in MeOH) (J&K Scientific, Germany) was diluted with ultrapure water for LC-MS/MS measurements.

Potassium dihydrogen phosphate and dipotassium hydrogen phosphate (Macklin, USA), were diluted in DI water to prepare a 100 mmol/L phosphate buffer (PB, pH=7.0). The specific surface area and average pore width distribution of zeolite (Si:Al = 2.5:1, Macklin, USA) were determined by a specific surface area and pore width analyzer (ASAP2460, McMurraytec, USA) (Appendix A **Table S1**), the zeta potential of zeolite in 100 mM PB (pH=7.0) was determined by a zeta potential analyzer (ZS90, Malvern, UK) with disposal folded capillary cells.

2.2 Analytical methods

PFOA was quantified by a LC-MS/MS system (6460 and 1290 Infinity, Agilent, USA), using a C18 column, (ZOBRAX RR Eclipse Plus, Agilent, USA). Methanol and 10 mmol/L ammonium acetate were mixed as the mobile phase, following a time-dependent gradient as listed in Appendix A **Table S2**. Multiple reaction monitoring and electron spray ionization modes were adopted to quantify PFOA. Calibration curves (0.01-0.1, 0.1-1.0, and 1.0-10 mg/L, cf. Appendix A **Fig. S1**) were established at the beginning of each measurement batch with standards, batch samples ≤ 50 and $R^2 \geq 0.999$ were required to control data quality.

2.3 Kinetics of PFOA sorption in percolation systems

Electrokinetic percolation columns adopted from our previous work (Shan et al., 2018) were settled in a water bath with temperature-conditioning (DLSB 5L/10, Yuhua, China) for kinetic experiments (Appendix A **Fig. S2**). Zeolite was washed 3 times with de-ionized water and dried for 12 h at 80˚C in the oven and kept in a vacuum desiccator till use. The electrokinetic apparatus was wet-packed with 6 g zeolite in PB. Two disc-shaped Ti/Ir electrodes at the top (cathode) and bottom (anode) of the column were connected to a DC power pack (IT6720, Itech, China) to produce electric field strengths X = 1, 2, and 3 V/cm, resulting in stable direct currents of 0.03 A, 0.06 A, and 0.09 A, respectively. Then 10 mg/L PFOA in PB electrolyte was pumped through the column under static temperatures of 10, 20, 30, 40, and 50□ with deviations ≤ 2°C. 1 mL liquid was sampled before and after percolation at given time intervals up to 48 hr. After centrifugation at 5000 x *g*, the supernatant was measured with LC-MS/MS. Each experiment was conducted in triplicate.

Breakthrough curves and the mass of PFOA accumulating on zeolite under varying DC electric field strengths and temperatures can be depicted by the PFOA concentration shifting over sorption time.

2.4 Isotherm PFOA sorption experiments

Isotherm batch experiments were conducted in PB in sealed 15 mL polypropylene centrifuge tubes at a sorbent-to-liquid ratio of 1:1000 (g/mL), with 8 initial PFOA concentrations ranging from 1 to 8 mg/L. Zeolite and liquids in the centrifuge tubes were equilibrated in a horizontal shaker with temperature conditioning (HNYC-211C, Ounuo, China) at 150 r/min for 7 days at temperatures of 10 °C, 20 °C, 30 °C, 40 °C, and 50°C, with fluctuations < 2 °C. Zeolite particles were ground into a fine powder with an average particle diameter of 74 ± 4 μm to shorten the equilibrium time, the powder zeolite was only used in isothermal experiments. After equilibrating for 7 days, liquid-zeolite suspensions were centrifuged at 5000 × *g* for 10 min, 1 mL samples were taken by a syringe gently from the supernatant and measured by LC-MS/MS. Each experiment was conducted in triplicate.

2.5 Calculation of EOF velocities

EOF velocity (v_{EOF}) in a pore of radius r (Vallano and Remcho, 2000) was quantified by the maximum v_{EOF} ($v_{EOF,max}$) and a function ($f(\kappa r)$, which includes electrical double layer and pore radius effects (Rice and Whitehead, 1965) (eqs. 1-3)

$$v_{EOF} = v_{EOF,\max} * f(\kappa r) \tag{1}$$

$$v_{EOF,\max} = -\frac{\varepsilon_r \varepsilon_0 X \xi}{\eta} \tag{2}$$

$$f(\kappa r) = \left(1 - \frac{2I_1(\kappa r)}{\kappa r I_0(\kappa r)}\right) \tag{3}$$

where I_0 is the modified Bessel function zero order, I_1 is the modified Bessel function of the first order, κ is the reciprocal of the electrical double layer thickness (1/m) (Sharma and Hanumantha Rao, 2003), and r is the intra-particle pore radius of zeolite (m). ε_r is the dielectric constant, ε_0 is the vacuum permittivity (F/m), η is the liquid viscosity (Pa s), ξ is the zeta potential of zeolite (V), and X is the DC field strength (V/m).

2.6 Kinetic and isotherm models

2.6.1. Kinetic equations

Sorption kinetic is the rate of PFOA adsorbed onto zeolite. It can be analyzed by mathematical models including the intra-particle model (eq. 4), the pseudo-first-order (PFO) model (eq. 5), and the pseudo-second-order (PSO) model (eq. 6).

The linearized expression of the intra-particle diffusion model (Lei et al., 2022) is

$$q_t = k_p t^{1/2} + C \tag{4}$$

where k_p (mg/g/min$^{1/2}$) is the kinetic constant of the intra-particle diffusion model and C (mg/g) is a constant.

In the PFO model (Yu et al., 2009) the q_e and q_t are the adsorbate concentration in the sorbent at equilibrium and at time t (1/hr), respectively; k_{PFO} is the kinetic constant.

$$\ln(q_e - q_t) = -k_{PFO} t + \ln q_e \tag{5}$$

The PSO model can be described by the equation with k_{PSO} being the PSO kinetic constant (g/mg/hr).

$$\frac{t}{q_t} = \left(\frac{1}{q_e}\right) t + \frac{1}{k_{PSO} q_e^{\,2}} \tag{6}$$

2.6.2. Isotherm equations

Sorption isotherms describe the relationship between the amount of PFOA adsorbed onto zeolite and the concentration of the adsorbate in the liquid at a constant temperature. Sorption isotherms were analyzed by the Freundlich model and the Langmuir model (Tran et al., 2017). The Langmuir approach can be described by the equation

$$q_e = \frac{Q_{\max} K_L C_e}{1 + K_L C_e} \tag{7}$$

where Q_{max} is the max sorption capacity at sorption equilibrium, K_L is the Langmuir constant, C_e is the PFOA concentration in liquid (mg/L). The Freundlich model is described by eq. 8, where K_F refers to the Freundlich constant ((mg/g)/ (mg/L)^n).

$$q_e = K_F C_e^{\,n} \tag{8}$$

3. Results and Discussion

3.1 Electrokinetic and temperature effects on PFOA sorption to zeolite

Heating and electrokinetics both decreased PFOA sorption on zeolite. Cumulative PFOA mass thereby showed a bi-phasic behavior with a fast initial increase until ca. t = 14 hr followed by reduced mass accumulation increment rate thereafter (**Fig. 1**). In the absence of DC, heating from 10 °C to 50 °C decreased PFOA loading from 10.1 mg to 7.6 mg (≈25% reduction) at t = 48 hr. A similar trend was found in the presence of DC, where heating from 10 °C to 50 °C decreased sorbed PFOA mass at all electric field strengths applied; e.g., after 48 hr at X = 1 V/cm from 9.4 mg to 7.4 mg (21%), at X = 2 V/cm from 8.7 mg to 7.2 mg (17%) at X = 2 V/cm, and at X = 3 V/cm from 8.1 mg to 6.7 mg (17%). At any temperature tested, the application of DC fields likewise decreased PFOA loading to zeolite; for instance, after 48 hr at X = 3 V/cm by 20% at 10 °C, 15% at 20 °C, 15% at 30°C, 14% at 40 °C, and 12% at 50 °C, respectively. Although PFOA may mostly be ionized (Goss, n.d.) at pH = 7, observed electrokinetic effects on PFOA sorption are in accordance with previous research on non-ionic phenanthrene sorption on mineral sorbents revealing reduced v_{EOF}-dependent phenanthrene sorption to zeolites in presence of DC electric fields (Shan et al., 2020b). This shows that electrokinetic phenomena have reduced the availability of PFOA molecules to e.g., intraparticle zeolite sorption sites. The good correlation of the observed effects to v_{EOF} further suggests that EOF is a good predictor for electrokinetic sorption effects of anionic ambiphilic compounds such as PFOA where interactions of the hydrophobic fluorocarbon part may drive its sorption rates (Yu et al., 2009). Our study further extends our knowledge on the effect of temperature on electrokinetic effects on contaminant sorption[46] and, hence, allows us to apply heating and electrokinetic phenomena as drivers for contaminant sorption in future technological applications.

3.2 Electrokinetic and temperature effects on PFOA sorption kinetics

Sorption kinetics were further analyzed by fitting the time-dependent sorption data to the pseudo-first-order (PFO), intra-particle diffusion and pseudo-second-order (PSO) models (Ho et al., 2000; Morelis and van Noort, 2008). The regression correlations proposed the

PSO model to better describe sorption kinetics ($R^2 \geq 0.96$) than the PFO model ($0.89<R^2<0.99$) or the intra-particle model ($0.74<R^2<0.91$) (**Fig. 2**, **Table 1,** Appendix A **Tables S3 & S4**). The kinetic constant of PSO (k_{PSO}) hence enabled us to compare PFOA sorption kinetics at the different temperatures and electrokinetic conditions tested. Increasing k_{PSO} (10^{-3} $g_{zeolite}/mg_{PFOA}/h$) thereby points at decreasing PFOA mass sorbing. Heating from 10 to 50 °C in the absence of DC increased the k_{PSO} from 256 $*10^{-3}$ g/mg/hr to 920 $*10^{-3}$ g/mg/hr (259%) in the absence of electric fields. In presence of DC, k_{PSO} increased between 10 °C and 50 °C by 143% (X = 1 V/cm), 91% (X = 2 V/cm), and 42% (X = 3 V/cm) (**Fig. 2, Table 1,** Appendix A **S3,**). Observed temperature-induced increases of k_{PSO} at a given electric field strength were lower at X = 3 V/cm (25%) than at X = 2 V/cm (59%), X = 1 V/cm (99%), and X = 0 V/cm (218%) (**Fig. 2, Table 1**, Appendix A **Fig. S3**, **Tables S3 & S4**).

Both heating and DC electric fields hence resulted in increased k_{PSO}, i.e., reduced PFOA sorption and enhanced PFOA transport, respectively (**Fig. 3**, Appendix A **Fig. S4**). The kinetic model analysis developed our previous work from a time point analysis to the sorption kinetics over 48 hr. It also provided an appropriate parameter to quantitatively depict electrokinetic effects on sorption kinetics and enabled comparisons between the heating effect and the electrokinetic effects over time shifting (Qin et al., 2015; Shan et al., 2020b).

3.3 Synergism of electrokinetic and heating effects on PFOA sorption

Our data propose that electrokinetic transport phenomena at the liquid-sorbent interface may influence sorption kinetics. The v_{EOF} has been discussed to be key to DC field effects on the sorption of non-ionic phenanthrene at room temperature (Shan et al., 2020b). We here further studied drivers of DC field effects at different temperatures on anionic, yet partially hydrophobic PFOA. To do so, we first quantified v_{EOF} in intra-particle pores of zeolite under various temperatures and DC field strengths by equations 5-7, using experimentally determined average pore width, and zeta potential of the zeolite sorbent. The temperature-controlled sorption capacity was investigated by the sorption equilibrium experiments, and analyzed by Freundlich and Langmuir equations (eqs. 7-8). Calculated v_{EOF} and isothermal parameters K_F and K_L were subsequently correlated to the

experimentally derived kinetic constants (k_{PSO}).

Regression correlation showed that the v_{EOF} and the k_{PSO} were highly linearly correlated at all temperatures, with $R^2 > 0.96$ (**Fig. 4A,** Appendix A **Table S5**), suggesting that EOF was an apparent driver for observed PFOA sorption kinetic variations. The slope values were positive, indicating that increasing v_{EOF} resulted in higher k_{PSO}, and, subsequently, decreased PFOA sorption to zeolite in DC fields. DC effects thereby were significantly (>500%) higher at 10˚C as compared to 50˚C (**Table 2, Fig. 4A**) indicating the synergetic effects of heating and DC fields on PFOA sorption rates (**Fig. 4B**).

Linking the slope values (derived from linear v_{EOF}-k_{PSO} fitting) with either the Langmuir or Freundlich parameters showed a positive apparent quadratic correlation with $R^2 = 0.996$ for K_L and 0.955 for K_F (**Fig. 4B**). This suggests that K_L may be used to estimate temperature DC-temperature effects on PFOA sorption on zeolites. Decreasing K_L at higher temperatures thus promotes DC field effects on PFOA sorption to zeolite; i.e. a combination of high temperature and high DC field strength leads to less sorption and higher PFOA transport. Such observation is in line with previous research revealing that heating varies the sorption capacity, which in turn may also affect the sorption kinetics(Qu et al., 2009; Yang et al., 2018).

Based on the apparent correlations, we further developed an approach to describe and predict the temperature-dependent electrokinetic effects on PFOA sorption. The approach combines v_{EOF} (as a factor reflecting the presence of DC electric field), liquid viscosity (as a factor reflecting the influence of temperature), and their joint impact on the kinetic constant k_{PSO} (**Fig. 5**). At low liquid viscosity (e.g. at lower T) and high v_{EOF} (e.g. at elevated X) strongly reduced PFOA sorption, i.e. enhanced PFOA transport through zeolite is evidenced. By contrast, at high viscosity and low v_{EOF}, poor PFOA through zeolite is calculated. Such temperature (i.e. liquid viscosity) dependent correlation extends previous approaches to compare DC field effects on the sorption of a hydrophobic contaminant (phenanthrene) to geo-sorbents(Shan et al., 2020b). Although PFOA in our system may be mobilized both by electromigration and EOF, it further reveals that v_{EOF} nevertheless may be a good descriptor for DC field effects on PFOA sorption and transport in the geo-sorbent zeolite.

3.4 Relevance for environmental and biotechnological applications

Our results reveal that temperature and electrokinetic effects control the sorption kinetics and concomitant transport of PFOA in the geo-sorbent zeolite. Electrokinetic techniques hence may be promising to regulate PFOA-sorbent interactions. Our approach may also be used to kinetically regulate the interaction of other contaminants and zeolite-like sorbents in the manmade/natural environmental (bio-)technology (Qin et al., 2015; Shan et al., 2018). Enhanced PFOA transport may reduce time and subsequent costs of physical-chemical removal processes (e.g., permeable reactive barrier) around point source pollution sites (Ma et al., 2022; Shojaei et al., 2021). As sorption effects in DC fields are temperature dependent, our data further suggest that both the electric field strength and/or the temperature of a given system can be adjusted to the transport needs for PFOA. In summer, for instance, higher environmental temperatures may require lower DC field strengths as in winter, where moderate heating may promote PFOA transport rates. Soil matrices typically consist of a mixture of mineral and carbonaceous materials (Gill et al., 2014; Wick et al., 2007), considering previously investigated mechanisms of electrokinetic-controlled phenanthrene sorption on several carbonaceous sorbents (Qin et al., 2015; Shan et al., 2020b), the temperature-controlled electrokinetic approaches may enhance both hydrophobic and hydrophilic chemical transport through mineral contents in the soil. Such an approach may also elevate the transport, of a wide range of other similar contaminants in zeolite-type geo-matrices, thereby promoting efficient transport to treatment zones and so reducing the threat to the environment and human health. This may give rise to future technical applications, which allow regulating sorption processes, for instance in response to fluctuating adsorbate concentrations in contaminated water streams, in electro-bioremediation, or to avoid unwanted sorption solutes in technical applications.

Acknowledgment

The authors would like to thank the financial support from the National Natural Science Foundation of China (Grant No. 42277011), and the fellowship of the China Postdoctoral Science Foundation (2023T160667 & 2022M713300).

Appendix A. Supplementary data

Supplementary data associated with this article can be found in the online version at xxxxxx.

References

Benninghoff, A.D., Orner, G.A., Buchner, C.H., Hendricks, J.D., Duffy, A.M., Williams, D.E., 2012. Promotion of Hepatocarcinogenesis by Perfluoroalkyl Acids in Rainbow Trout. Toxicol. Sci. 125, 69–78. https://doi.org/10.1093/toxsci/kfr267

Cousins, I.T., Johansson, J.H., Salter, M.E., Sha, B., Scheringer, M., 2022. Outside the Safe Operating Space of a New Planetary Boundary for Per- and Polyfluoroalkyl Substances (PFAS). Environ. Sci. Technol. 56, 11172–11179. https://doi.org/10.1021/acs.est.2c02765

Do, D.D., 1998. Adsorption analysis: equilibria and kinetics, Series on chemical engineering. Imperial College Press, London.

Elimelech, M., Gregory, J., Jia, X., Williams, R.A., 1995. Particle Deposition and Aggregation, in: Particle Deposition and Aggregation. Elsevier, pp. xiii–xv. https://doi.org/10.1016/B978-0-7506-0743-8.50004-2

Flores, C., Ventura, F., Martin-Alonso, J., Caixach, J., 2013. Occurrence of perfluorooctane sulfonate (PFOS) and perfluorooctanoate (PFOA) in N.E. Spanish surface waters and their removal in a drinking water treatment plant that combines conventional and advanced treatments in parallel lines. Sci. Total Environ. 461–462, 618–626. https://doi.org/10.1016/j.scitotenv.2013.05.026

Ganbat, N., Altaee, A., Zhou, J.L., Lockwood, T., Al-Juboori, R.A., Hamdi, F.M., Karbassiyazdi, E., Samal, A.K., Hawari, A., Khabbaz, H., 2022. Investigation of the effect of surfactant on the electrokinetic treatment of PFOA contaminated soil. Environ. Technol. Innov. 28, 102938. https://doi.org/10.1016/j.eti.2022.102938

Ghosal, S., 2004. Fluid mechanics of electroosmotic flow and its effect on band broadening in capillary electrophoresis. ELECTROPHORESIS 25, 214–228. https://doi.org/10.1002/elps.200305745

Gill, R.T., Harbottle, M.J., Smith, J.W.N., Thornton, S.F., 2014. Electrokinetic-enhanced bioremediation of organic contaminants: a review of processes and environmental applications. Chemosphere 107, 31–42. https://doi.org/10.1016/j.chemosphere.2014.03.019

Goss, K.-U., 2008. The pK_a Values of PFOA and Other Highly Fluorinated Carboxylic Acids. Environ. Sci. Technol. 42, 456–458. https://doi.org/10.1021/es702192c

Goss, K.-U., n.d. The pKa Values of PFOA and Other Highly Fluorinated Carboxylic Acids 3.

Grimes, B.A., Meyers, J.J., Liapis, A.I., 2000. Determination of the intraparticle electroosmotic volumetric flow-rate, velocity and Peclet number in capillary electrochromatography from pore network theory. J. Chromatogr. A 890, 61–72. https://doi.org/10.1016/S0021-9673(00)00130-8

Ho, Y.S., Ng, J.C.Y., McKay, G., 2000. KINETICS OF POLLUTANT SORPTION BY BIOSORBENTS: REVIEW. Sep. Purif. Methods 29, 189–232. https://doi.org/10.1081/SPM-100100009

Hoffman, K., Webster, T.F., Weisskopf, M.G., Weinberg, J., Vieira, V.M., 2010. Exposure to Polyfluoroalkyl Chemicals and Attention Deficit/Hyperactivity Disorder in U.S. Children 12–15 Years of Age. Environ. Health Perspect. 118, 1762–1767. https://doi.org/10.1289/ehp.1001898

Hunter, R.J., 2013. Zeta potential in colloid science: principles and applications. Academic press.

Jeon, J., Kannan, K., Lim, H.K., Moon, H.B., Ra, J.S., Kim, S.D., 2010. Bioaccumulation of Perfluorochemicals in Pacific Oyster under Different Salinity Gradients. Environ. Sci. Technol. 44, 2695–2701. https://doi.org/10.1021/es100151r

Kar, A., Chiang, T.-Y., Rivera, I.O., Sen, A., Velegol, D., 2016. Correction to Enhanced Transport into and out of Dead-End Pores. ACS Nano 10, 3871–3871. https://doi.org/10.1021/acsnano.6b00965

Kopinke, F.-D., Georgi, A., Goss, K.-U., 2018. Comment on “Mistakes and inconsistencies regarding adsorption of contaminants from aqueous solution: A critical review, published by Tran et al. [Water Research 120, 2017, 88–116].” Water Res. 129, 520–521. https://doi.org/10.1016/j.watres.2017.09.055

Lee, T.C., Keh, H.J., 2014. Electrophoretic motion of a charged particle in a charged cavity. Eur. J. Mech. - BFluids 48, 183–192. https://doi.org/10.1016/j.euromechflu.2014.06.004

Lee, Y.-F., Huang, Y.-F., Tsai, S.-C., Lai, H.-Y., Lee, E., 2016. Electrophoretic and Electroosmotic Motion of a Charged Spherical Particle within a Cylindrical Pore Filled with Debye–Bueche–Brinkman Polymeric Solution. Langmuir 32, 13106–13115. https://doi.org/10.1021/acs.langmuir.6b02795

Lei, X., Yao, L., Lian, Q., Zhang, X., Wang, T., Holmes, W., Ding, G., Gang, D.D., Zappi, M.E., 2022. Enhanced adsorption of perfluorooctanoate (PFOA) onto low oxygen content ordered mesoporous carbon (OMC): Adsorption behaviors and mechanisms. J. Hazard. Mater. 421, 126810. https://doi.org/10.1016/j.jhazmat.2021.126810

Lein, N.P.H., Fujii, S., Tanaka, S., Nozoe, M., Tanaka, H., 2008. Contamination of perfluorooctane sulfonate (PFOS) and perfluorooctanoate (PFOA) in surface water of the Yodo River basin (Japan). Desalination 226, 338–347. https://doi.org/10.1016/j.desal.2007.01.247

Lindim, C., Cousins, I.T., vanGils, J., 2015. Estimating emissions of PFOS and PFOA to the Danube River catchment and evaluating them using a catchment-scale chemical transport and fate model. Environ. Pollut. 207, 97–106. https://doi.org/10.1016/j.envpol.2015.08.050

Lorber, M., Eaglesham, G.E., Hobson, P., Toms, L.-M.L., Mueller, J.F., Thompson, J.S., 2015. The effect of ongoing blood loss on human serum concentrations of perfluorinated acids. Chemosphere 118, 170–177. https://doi.org/10.1016/j.chemosphere.2014.07.093

Ma, D., Zhong, H., Lv, J., Wang, Y., Jiang, G., 2022. Levels, distributions, and sources of legacy and novel per- and perfluoroalkyl substances (PFAS) in the topsoil of Tianjin, China. J. Environ. Sci. 112, 71–81. https://doi.org/10.1016/j.jes.2021.04.029

Morelis, S., van Noort, P.C.M., 2008. Kinetics of phenanthrene desorption from activated carbons to water. Chemosphere 71, 2044–2049. https://doi.org/10.1016/j.chemosphere.2008.01.048

Niarchos, G., Sörengård, M., Fagerlund, F., Ahrens, L., 2022. Electrokinetic remediation for removal of per- and polyfluoroalkyl substances (PFASs) from contaminated soil. Chemosphere 291, 133041. https://doi.org/10.1016/j.chemosphere.2021.133041

Probstein, R.F., 1994. Physicochemical hydrodynamics: an introduction, 2nd ed. ed. Wiley, New York.

Qian, L., Kopinke, F.-D., Scherzer, T., Griebel, J., Georgi, A., 2022. Enhanced degradation of perfluorooctanoic acid by heat-activated persulfate in the presence of zeolites. Chem. Eng. J. 429, 132500. https://doi.org/10.1016/j.cej.2021.132500

Qin, J., Moustafa, A., Harms, H., El-Din, M.G., Wick, L.Y., 2015. The power of power: Electrokinetic control of PAH interactions with exfoliated graphite. J. Hazard. Mater. 288, 25–33. https://doi.org/10.1016/j.jhazmat.2015.02.008

Qu, Y., Zhang, C., Li, F., Bo, X., Liu, G., Zhou, Q., 2009. Equilibrium and kinetics study on the adsorption of perfluorooctanoic acid from aqueous solution onto powdered activated carbon. J. Hazard. Mater. 169, 146–152. https://doi.org/10.1016/j.jhazmat.2009.03.063

Rice, C.L., Whitehead, R., 1965. Electrokinetic Flow in a Narrow Cylindrical Capillary. J. Phys. Chem. 69, 4017–4024. https://doi.org/10.1021/j100895a062

Rice, C.L., Whitehead, R., n.d. Electrokinetic Flow in a Narrow Cylindrical Capillary 8.

Shan, Y., Harms, H., Wick, L.Y., 2018. Electric Field Effects on Bacterial Deposition and Transport in Porous Media. Environ. Sci. Technol. 52, 14294–14301. https://doi.org/10.1021/acs.est.8b03648

Shan, Y., Liu, L., Liu, Y., Harms, H., Wick, L.Y., 2020a. Effects of Electrokinetic Phenomena on Bacterial Deposition Monitored by Quartz Crystal Microbalance with Dissipation Monitoring. Environ. Sci. Technol. 54, 14036–14045. https://doi.org/10.1021/acs.est.0c04347

Shan, Y., Qin, J., Harms, H., Wick, L.Y., 2020b. Electrokinetic effects on the interaction of phenanthrene with geo-sorbents. Chemosphere 242, 125161. https://doi.org/10.1016/j.chemosphere.2019.125161

Sharma, P.K., Hanumantha Rao, K., 2003. Adhesion of Paenibacillus polymyxa on chalcopyrite and pyrite: surface thermodynamics and extended DLVO theory. Colloids Surf. B Biointerfaces 29, 21–38. https://doi.org/10.1016/S0927-7765(02)00180-7

Shi, L., Harms, H., Wick, L.Y., 2008. Electroosmotic Flow Stimulates the Release of Alginate-Bound Phenanthrene. Environ. Sci. Technol. 42, 2105–2110. https://doi.org/10.1021/es702357p

Shojaei, M., Kumar, N., Chaobol, S., Wu, K., Crimi, M., Guelfo, J., 2021. Enhanced Recovery of Per- and Polyfluoroalkyl Substances (PFASs) from Impacted Soils Using Heat Activated Persulfate. Environ. Sci. Technol. 55, 9805–9816. https://doi.org/10.1021/acs.est.0c08069

Sprocati, R., Rolle, M., 2022. On the interplay between electromigration and electroosmosis during electrokinetic transport in heterogeneous porous media. Water Res. 213, 118161. https://doi.org/10.1016/j.watres.2022.118161

Tran, H.N., You, S.-J., Hosseini-Bandegharaei, A., Chao, H.-P., 2017. Mistakes and inconsistencies

regarding adsorption of contaminants from aqueous solutions: A critical review. Water Res. 120, 88–116. https://doi.org/10.1016/j.watres.2017.04.014

Tsang, H., Cheung, T.-Y., Kodithuwakku, S.P., Chai, J., Yeung, W.S.B., Wong, C.K.C., Lee, K.-F., 2013. Perfluorooctanoate suppresses spheroid attachment on endometrial epithelial cells through peroxisome proliferator-activated receptor alpha and down-regulation of Wnt signaling. Reprod. Toxicol. 42, 164–171. https://doi.org/10.1016/j.reprotox.2013.08.001

Vallano, P.T., Remcho, V.T., 2000. Modeling Interparticle and Intraparticle (Perfusive) Electroosmotic Flow in Capillary Electrochromatography. Anal. Chem. 72, 4255–4265. https://doi.org/10.1021/ac0005969

Wen, D., Fu, R., Li, Q., 2021. Removal of inorganic contaminants in soil by electrokinetic remediation technologies: A review. J. Hazard. Mater. 401, 123345. https://doi.org/10.1016/j.jhazmat.2020.123345

Wick, L.Y., Shi, L., Harms, H., 2007. Electro-bioremediation of hydrophobic organic soil-contaminants: A review of fundamental interactions. Electrochimica Acta 52, 3441–3448. https://doi.org/10.1016/j.electacta.2006.03.117

Yang, Y., Ding, Q., Yang, M., Wang, Y., Liu, N., Zhang, X., 2018. Magnetic ion exchange resin for effective removal of perfluorooctanoate from water: study of a response surface methodology and adsorption performances. Environ. Sci. Pollut. Res. 25, 29267–29278. https://doi.org/10.1007/s11356-018-2797-1

Yu, Q., Zhang, R., Deng, S., Huang, J., Yu, G., 2009. Sorption of perfluorooctane sulfonate and perfluorooctanoate on activated carbons and resin: Kinetic and isotherm study. Water Res. 43, 1150–1158. https://doi.org/10.1016/j.watres.2008.12.001

List of Tables

Table 1. Kinetic parameters of the pseudo-second-order model at temperatures 10 - 50˚C and DC field strengths 0 - 3 V/cm.

Temperature	Pseudo-second-order parameters no DC			Pseudo-second-order parameters X = 1 V/cm			Pseudo-second-order parameters X = 2 V/cm			Pseudo-second-order parameters X = 3 V/cm		
(˚C)	q_e	k_{PSO} (10^{-3} g/mg/hr)	R^2	q_e	k_{PSO} (10^{-3} g/mg/hr)	R^2	q_e	k_{PSO} (10^{-3} g/mg/hr)	R^2	q_e	k_{PSO} (10^{-3} g/mg/hr)	R^2
10	0.35	256	0.98	0.29	401	0.98	0.24	573	0.98	0.21	815	0.98
20	0.28	426	0.98	0.24	563	0.98	0.22	735	0.98	0.20	845	0.98
30	0.25	547	0.98	0.22	704	0.98	0.20	853	0.98	0.18	1087	0.99
40	0.22	709	0.98	0.20	834	0.99	0.19	946	0.99	0.17	1129	0.99
50	0.20	920	0.98	0.19	975	0.99	0.18	1096	0.99	0.17	1154	0.99

Table 2. Regression results of isothermal and slopes of electroosmotic flow velocity (v_{EOF}) to the kinetic constant (k_{PSO}).

T	Slope	Freundlich Isotherm parameters			Langmuir Isotherm parameters		
(˚C)	S	K_F (mg/g)/(mg/L)^n	n	R^2	q_m (mg/g)	K_L (L/mg)	R^2
10	41	1072	0.78	0.99	6.3	220	0.99
20	24	933	0.80	1.00	5.9	200	0.99
30	24	871	0.80	1.00	5.6	200	0.99
40	15	724	0.80	1.00	5.5	180	0.99
50	8	692	0.80	1.00	5.3	160	1.00

List of figures

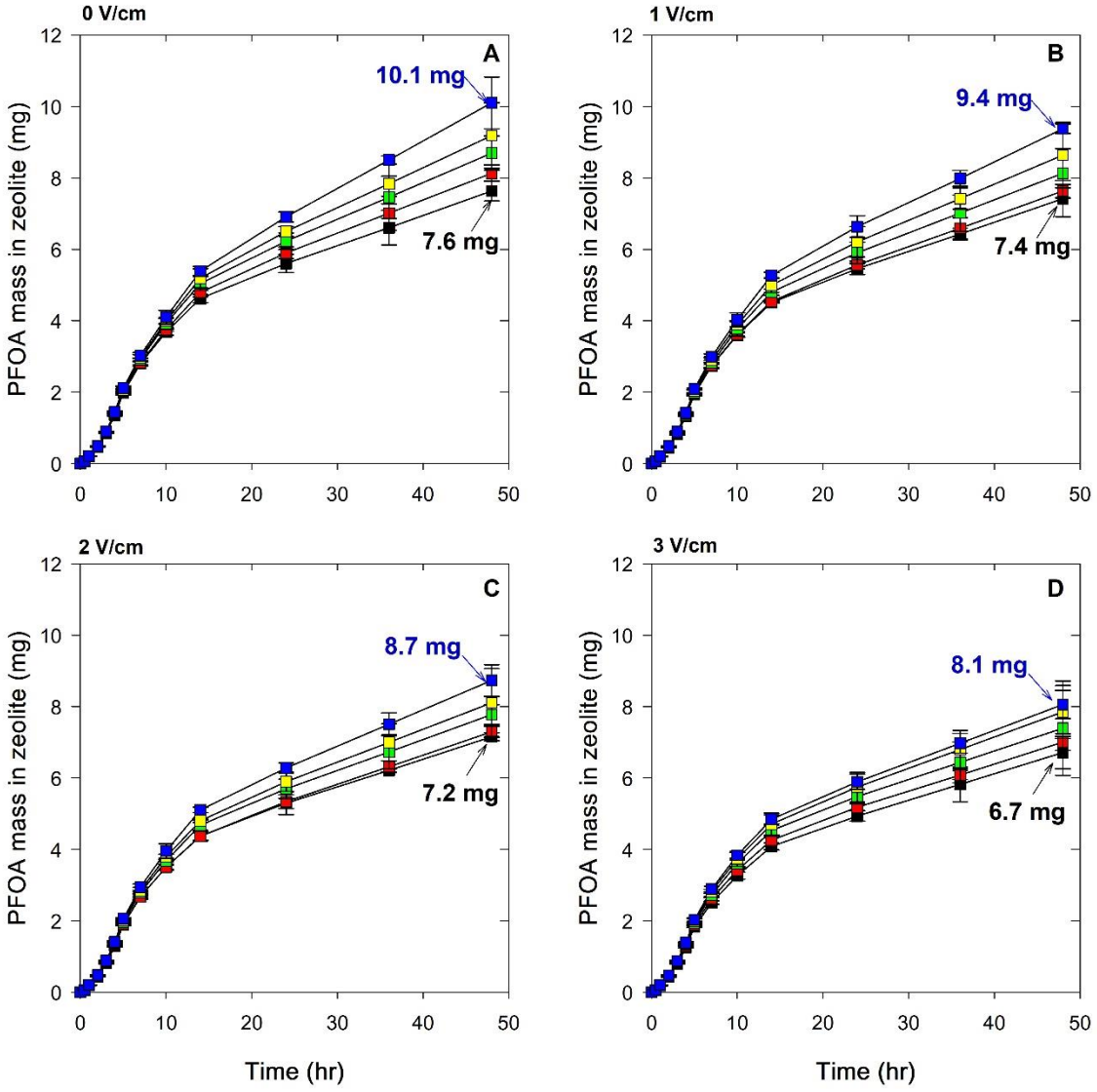

Figure 1. Perfluorooctanoic acid (PFOA) mass accumulated on zeolite under temperatures 10°C (blue), 20°C (yellow) 30°C (green), 40°C (red), and 50°C (black).

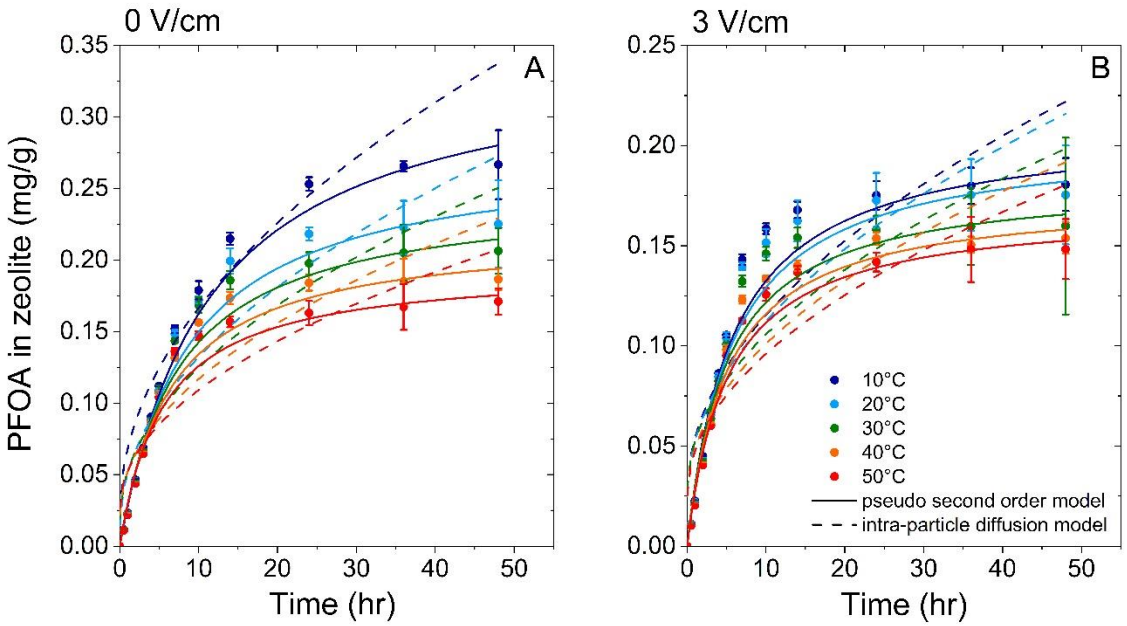

Figure 2. Effects of temperature (T = 10 - 50°C) on PFOA sorption kinetics DC field strengths of X = 0 (**Fig. 1A**) and 3 V/cm (**Fig. 1B**). The dashed and solid lines are the fitting curves of the intra-particle model and pseudo-second-order kinetic model, respectively.

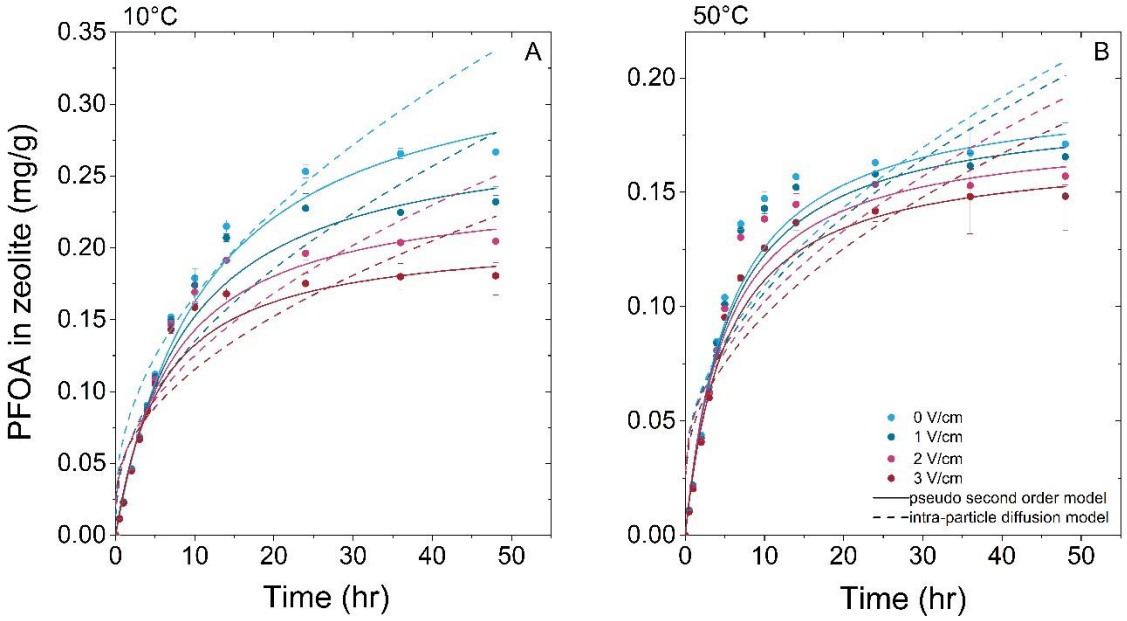

Figure 3. Effects of temperature (T = 10°C and 50°C) on sorption kinetics, with fitting curves of the intra-particle model and pseudo-second-order model, separately.

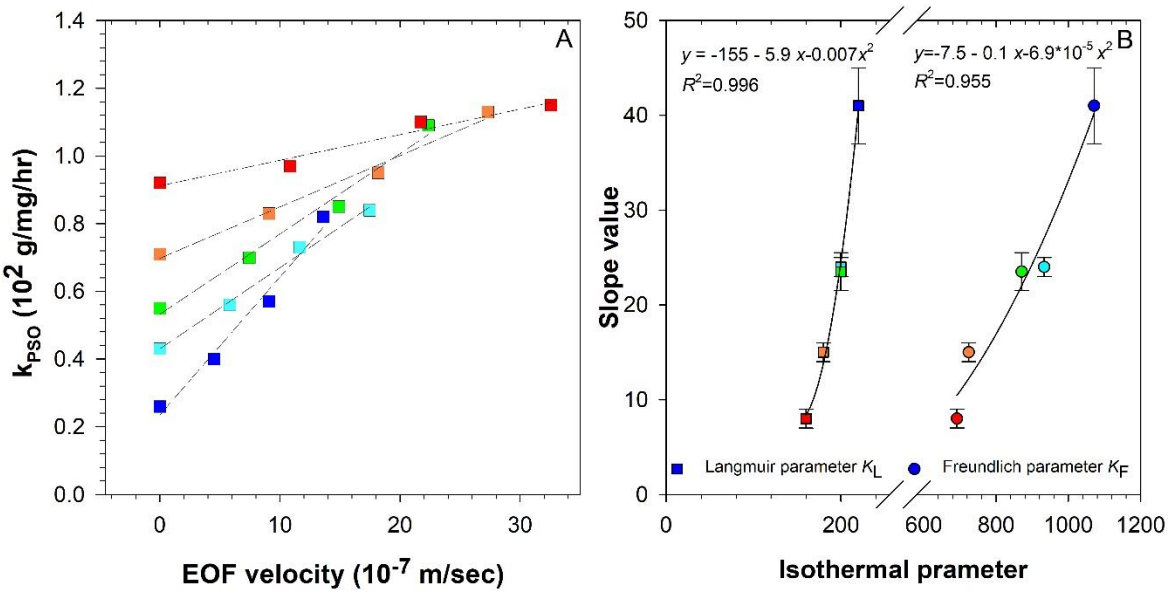

Figure 4. v_{EOF} correlation to the sorption kinetic constant (k_{PSO}) at T = 10°C (blue), 20°C (light blue), 30°C (green), 40°C (orange), 50°C (red) (**Fig. 4A**), and the derived slope values correlation with isothermal parameters (**Fig. 4B**).

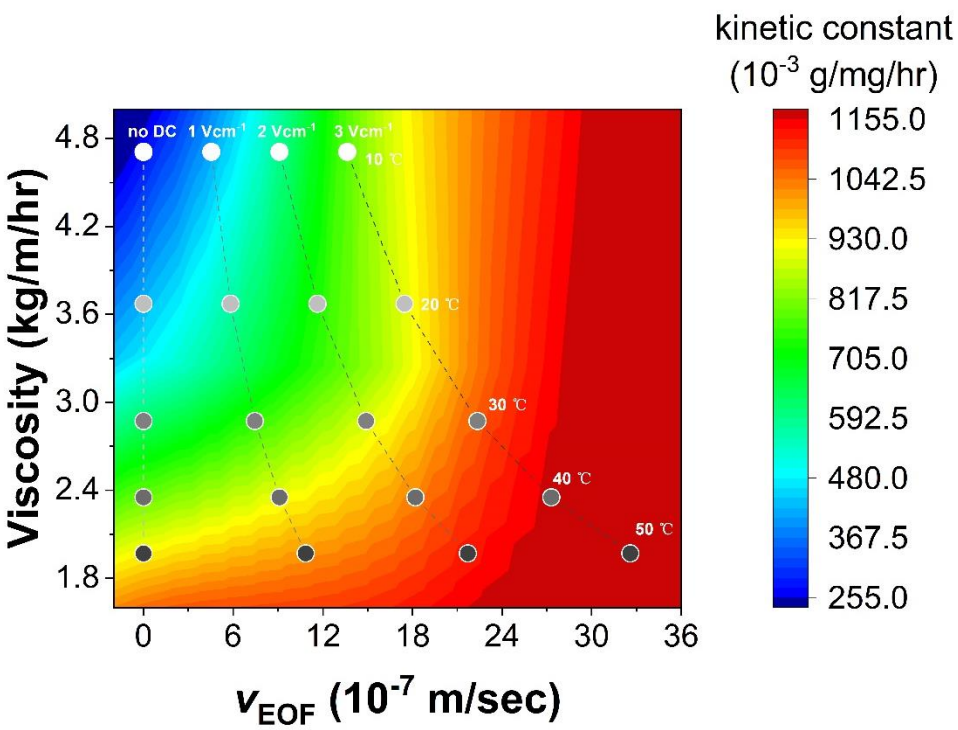

Figure 5. Interlinking between electroosmotic flow velocity ($v_{EOF,\ r}$), liquid viscosity (η), and their joint effects on PFOA sorption to zeolite. Warm colors reflect high k_{PSO}, i.e., decreased sorption, while cold colors reflect low k_{PSO}, i.e., increased sorption.